Supporting Information

Surface Oxidation under Ambient Air – Not Only a Fast and Economical Method to Identify Double Bond Positions in Unsaturated Lipids But Also a Reminder of Proper Lipid Processing

Ying Zhou[1§#], Hyejung Park[1§◊], Philseok Kim[2], Yan Jiang[1] and Catherine E. Costello[1]*

[1] Mass Spectrometry Resource, Department of Biochemistry, Boston University School of Medicine, Boston, MA 02118, USA

[2]Wyss Institute for Biologically Inspired Engineering and School of Engineering and Applied Sciences, Harvard University, Cambridge, MA 02138 USA

[#]Present address, Astra Zeneca-US, Waltham, MA

[◊]Present address, Genzyme Corporation, Waltham, MA

ABSTRACT: Additional information on tandem mass spectrometry experiments, roughness test of various surfaces, unsaturated fatty acid and phosphatidylcholine surface oxidation, N_2 protection and darkroom experiments and proposed structures of the CID MS fragments are provided.

Experimental methods.

Additional materials. Plates with Silica gel 60 HPTLC coated on aluminum or glass were purchased from EMD Chemicals Inc. (Gibbstown, NJ). Microscope glass slides and aluminum foils were purchased from Fisher Scientific (Pittsburgh, PA). All HPLC grade solvents were purchased from Merck (Darmstadt, Germany).

HPTLC. ST standards dissolved in $CHCl_3/CH_3OH$ (1:1, v/v) were applied by means of a microliter syringe (Hamilton Co., Reno, NV), as 3-mm spots on silica gel-coated plates. Plates for the analysis of acidic glycosphingolipids (GSLs) were developed with solvent system A ($CHCl_3/CH_3OH$/0.2% $CaCl_2$ (55:45:10, v/v/v)). The bovine brain total lipid extract was developed with solvent system B ($CHCl_3/CH_3OH/H_2O/CH_3COOH$ (90:50:5:2, v/v/v/v)). Duplicate spots of each lipid sample were deposited on a silica TLC plate and the plate was cut into two pieces after development. One piece was stained as a reference for the determination of the elution positions for the lipids of interest, and the other piece was used for TLC-MS analysis. Primuline staining reagent was applied for the detection of lipids.

Direct sampling TLC-MS. The liquid extraction surface analysis (LESA™) device for the TriVersa NanoMate (Advion BioSciences, Inc., Ithaca, NY) was coupled to the nanoESI source of a QSTAR Pulsar *i* Q-o-TOF MS (AB Sciex, Foster City, CA) that was operated in the negative ion mode. Typical LESA-MS experimental conditions were spray voltage, -1.5 kV; N_2 delivery gas pressure, 0.8 psi; and solvent system C ($(CH_3)_2CHOH/CH_3OH/H_2O$ (9:1:1, v/v/v)) as the extracting solvent mixture. A total volume of 8 μL of extracting solvent C was used for each extraction, with 6 μL being dispensed by a pipette tip held at 0.8 mm above the surface, to form a liquid-surface junction and facilitate liquid extraction of the analytes. The liquid junction was held in place for 1 s and then 1.5 μL of the solution was aspirated back into the tip. CID was performed with nitrogen gas to fragment the compounds of interest. The collision energy was set between -30 to -90 V, depending on the lipid structures. Typically, dissociation of singly-charged STs needed higher energy (~ -90 V) than multiply-charged gangliosides or singly-charged phospholipids (~ -50 V). The GD1a standard was employed for MS/MS calibration. Mass accuracy for the Q-Star Q-o-TOF MS in both MS and MS/MS modes was better than 15 ppm.

Characterization of surface roughness. The topography and roughness were characterized for samples deposited onto a microscope glass slide and the matte side of aluminum foil, using white light interferometry (Model NT-1100, Veeco) in the vertical scanning interferometry (VSI) mode with a 20X objective lens and a modulation threshold of 0.5%. A contact stylus profilometer (Model Dektak 6M, Veeco) with a load force of 5 mg was used for measuring the roughness of the silica TLC plate samples. At least three independent measurements were taken to calculate the average roughness (R_a) and standard deviation for all samples. The samples were also mounted on conductive carbon tape, sputter coated with gold, and examined with a Tescan Vega 3 scanning electron microscope.

Supplementary results and discussion.

Surface oxidation of fatty acids

In order to confirm that the surface lipid oxidation observed for ST is common to other lipid classes as well, stearic acid C18:0, oleic acid C18:1 (9*Z*), linoleic acid C18:2 (9*Z*, 12*Z*), lignoceric acid C24:0 and nervonic acid C24:1 (15*Z*) were examined on aluminum foil, since fatty acids represent the "simplest" lipids (Fig. S-9). No oxidation was observed on the saturated fatty acids (Fig. S-9a and 9d). Fig. S-9b shows the spectrum recorded for the products from oxidation of oleic acid after 1-h exposure to ambient air. $[M - H]^-$ ions were observed that corresponded to a shortened fatty acid containing a terminal aldehyde (*m/z* 171.10), or a second carboxyl moiety (*m/z* 187.10), as well as the residual intact starting material (*m/z* 281.25). Nervonic acid was also cleaved at its double bond position and showed signals at *m/z* 255.20, and 271.19 (Fig. S-9e). Because $[M – H]^-$ the aldehyde product of nervonic acid ($C_{15}H_{27}O_3^-$, *m/z* 255.1966) and the background palmitic acid ($C_{16}H_{31}O_2^-$, *m/z* 255.2330) are isobaric, the nervonic acid oxidation products were reanalyzed by FT-ICR MS to resolve these species and thereby remove any ambiguity regarding formation of the aldehyde (Fig. S-10). Over time, the abundances of the peaks corresponding to the aldehyde products were increased in the spectra and the intensities of their signals were compared to the signal from the remaining fatty acid (Fig. S-10b). The oxidation of linoleic acids resulted in the generation of only one set of products, observed at *m/z* 171.10, and 187.10 (Fig. S-9c) without the "step-by-step" cleavages reported by Harrison and Murphy for their OzID investigation of a phosphatidylcholine (PC) with multiple double bonds.[1] When the amount of oxidant is sufficient, both double bonds may react, at apparently similar rates, and be cleaved immediately and, as a result, the other small neutral pieces may not be detectable.

Interestingly, no ozonide was produced from these fatty acids. To check whether the ozonide is produced quickly, the fatty acids were deposited on aluminum foil and the formation of ozonides in the fatty acids was tracked for 5 min, 10 min, and 20 min by nanoESI-MS analysis with the TriVersa NanoMate. However, no such products were detected (data not shown). Since singlet oxygen reacts much faster on the isolated olefin, as discussed above, the fatty acids react more quickly with singlet oxygen than with ozone and the amount of the ozonides generated under these conditions might be undetectable. During ozone oxidation of carbon-carbon double bonds, primary ozonide formation is considered to be the rate-limiting step.[2,3] Furthermore, it is possible that, once formed, the ozonide is quickly cleaved. The cleavage may occur so rapidly that the ozonide intermediates cannot be detected. The presence of the aldehyde and carboxyl acid pair is sufficient to elucidate the original position of the double bond in fatty acids, even though no observed signal corresponds to the postulated ozonide intermediate.

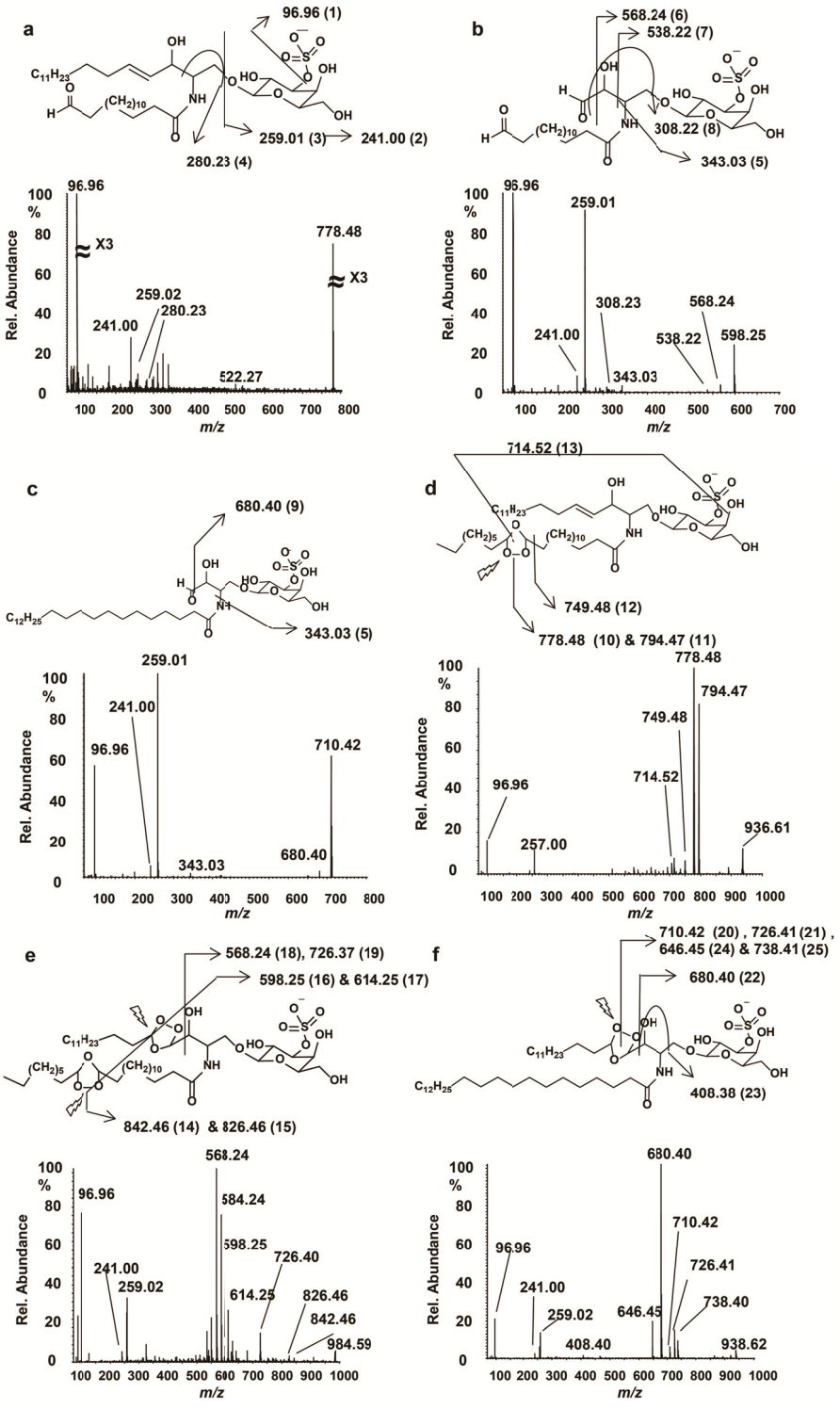

Figure S-1. CID MS/MS spectra recorded during TLC-MS experiments conducted in the negative-ion mode and assignments of the oxidation products from d18:1/C24:1 ST and d18:1/C24:0 ST. (a) CID of the precursor ion at *m/z* 778.5 that corresponds to the aldehyde formed on the fatty acid chain after oxidation of d18:1/C24:1 ST. (b) CID of the ion at *m/z* 598.3 that can be assigned as the di-aldehyde formed on both the fatty acid chain and the long chain

base of d18:1/C24:1 ST. (c) MS/MS spectrum obtained for the precursor ion at *m/z* 710.4 that can be assigned as the aldehyde formed at the double bond in the sphingoid base of d18:1/C24:0 ST. (d) CID MS/MS spectrum of *m/z* 936.6 corresponding to the ozonide formed at the double bond position in the fatty acyl chain of d18:1/C24:1 ST. (e) CID MS/MS spectrum of *m/z* 984.6 corresponding to di-ozonide formed on the double bonds in both the fatty acyl chain and the sphingoid base of d18:1/C24:1 ST. This spectrum was collected from the surface of aluminum foil after deposition of d18:1/C24:1 ST followed by exposure under ambient air after 1 hour. (f) CID MS/MS spectrum of the precursor ion *m/z* 938.6 assigned as the ozonide formed on the double bond in the long chain base of d18:1/C24:0 ST. Structures of the CID fragments are shown in the structure list in Figure S-11.

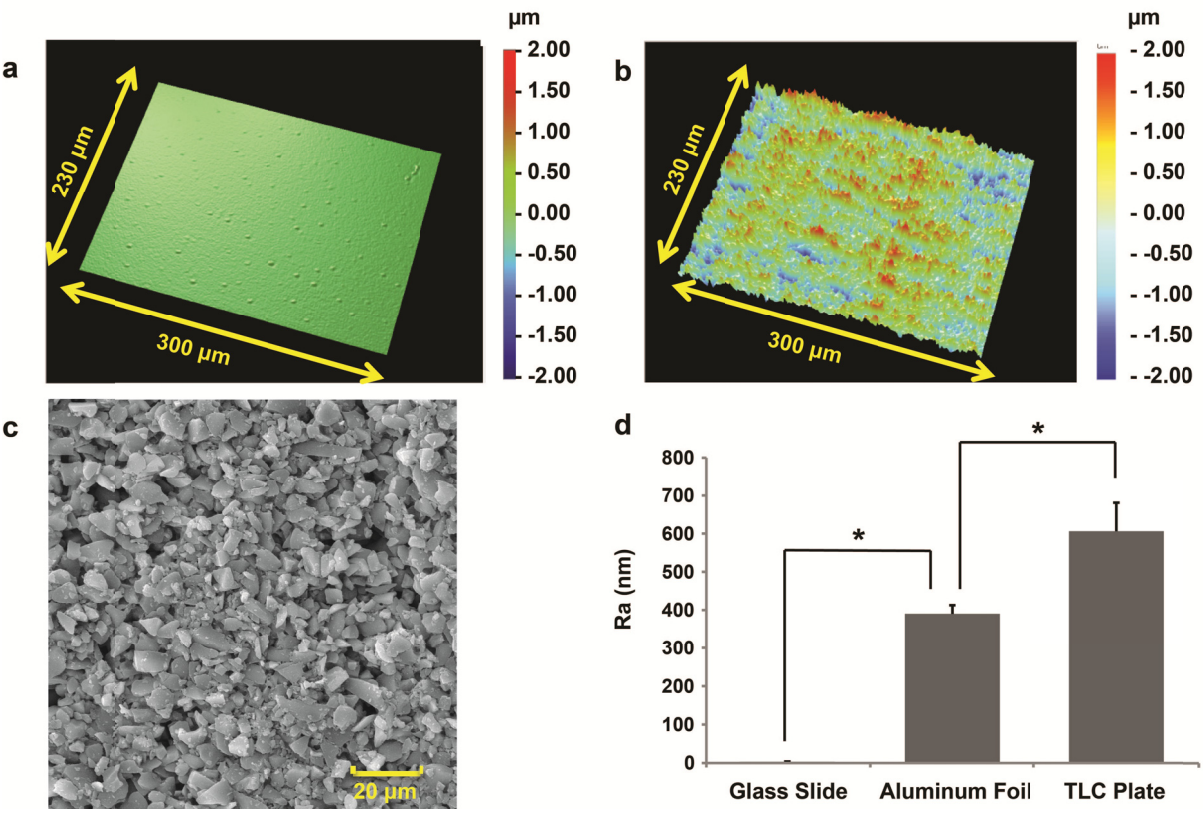

Figure S-2. Roughness test of various surfaces. The topography and roughness were characterized for samples deposited on a glass slide (a) and on the matte side of aluminum foil (b), using white light interferometry (Model NT-1100, Veeco) in the vertical scanning interferometry (VSI) mode with a 20X objective lens and a modulation threshold of 0.5%. A contact stylus profilometer (Model Dektak 6M, Veeco) with loading force of 5 mg was used for measuring the roughness of silica TLC plate samples. (c) At least three independent measurements were taken to calculate the average roughness (*Ra*) and standard deviation for all samples. The student's *t*-test was applied to determine the difference in roughness between groups. The roughness of the TLC plate was significantly more than the matte side of aluminum foil, while the roughness on the matte side of aluminum foil was significantly greater than the glass slide (d). (*) means $p < 0.05$.

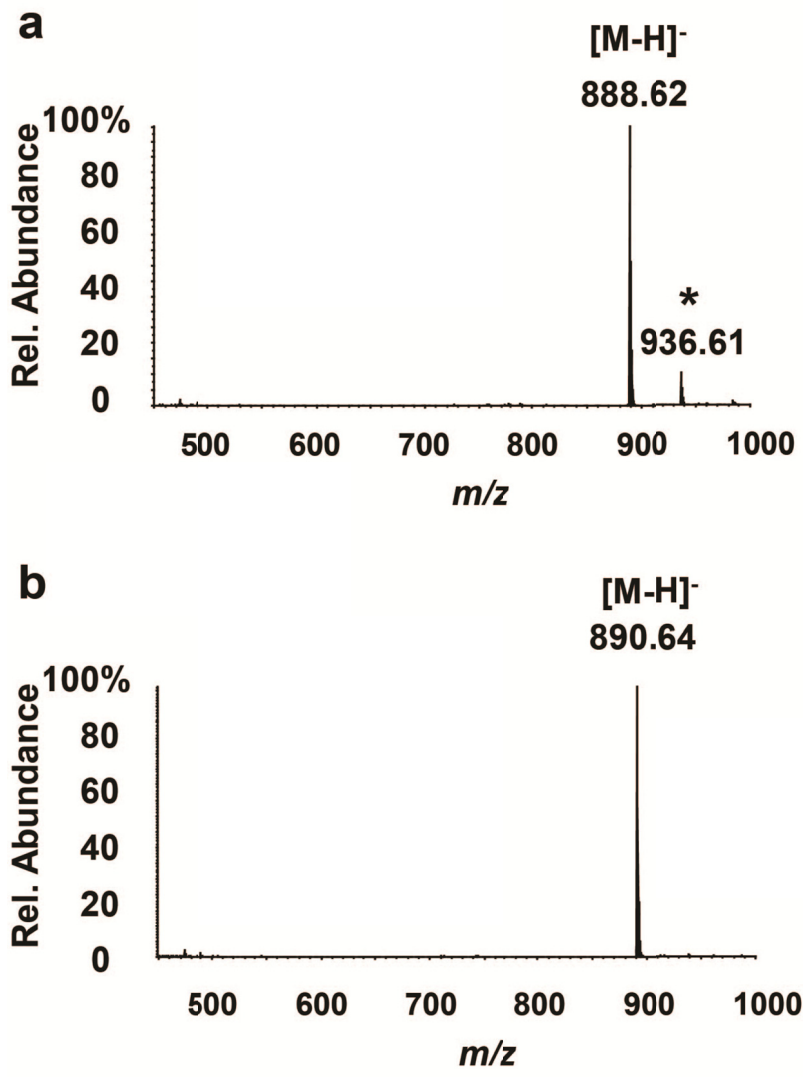

Figure S-3. Negative-ion mode ESI-MS spectra of d18:1/C24:1 ST (a) and d18:1/C24:0 ST (b) acquired following deposition onto aluminum foil and exposure to chemically generated ozone for 24 h. In the spectrum shown in (a), the $[M - H + 48]^-$ peak corresponding to an ozone adduct is marked with an asterisk (*).

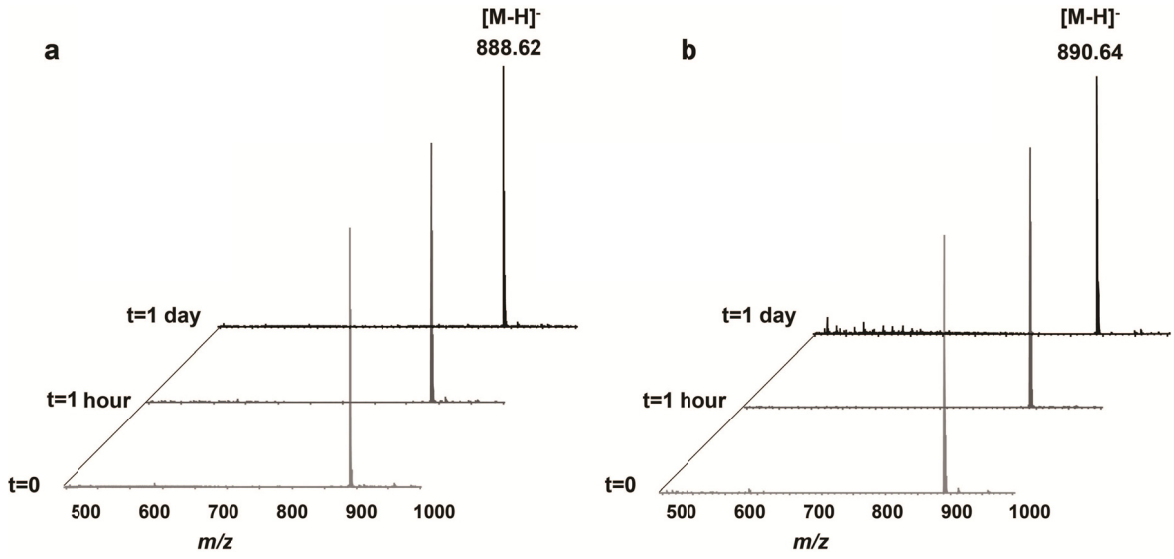

Figure S-4. ESI-MS spectra of (a) d18:1/C24:1 ST and (b) d18:1/C24:0 ST recorded for samples deposited on aluminum foil and kept under gaseous N_2 protection at times 0, 1 h and 1 day. One hundred pmol of each sample was deposited onto the aluminum foil, which had been placed into a three-necked flask. N_2 was purged into the flask to protect the sample from the ambient air. STs were extracted using the solvent mixture isopropyl alcohol/methanol/water (9:1:1, v/v/v) and were directly analyzed by ESI-MS.

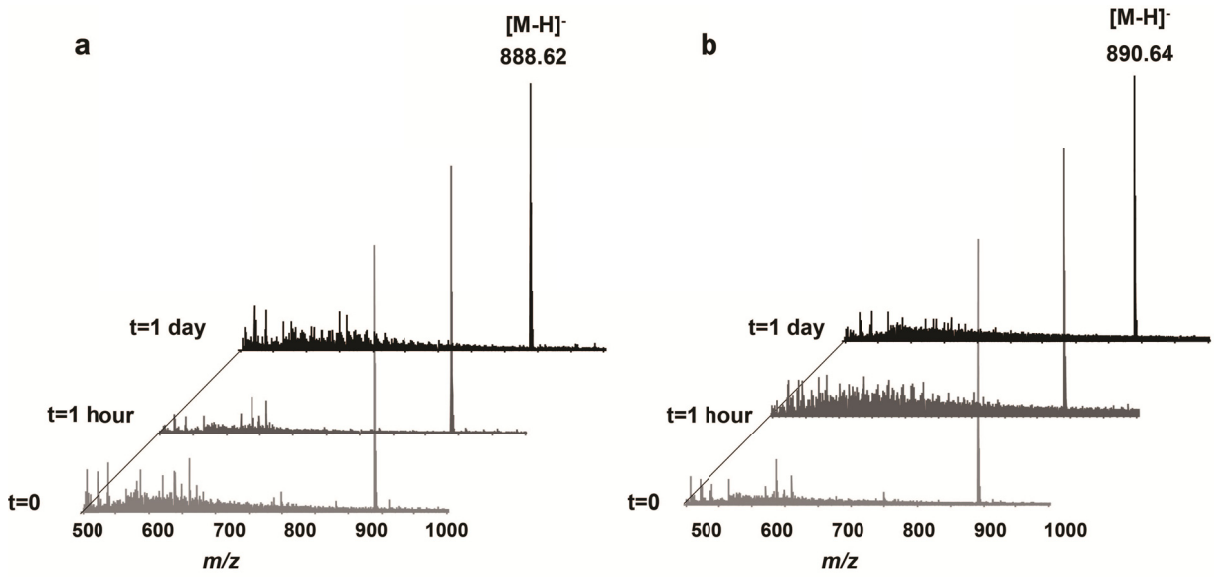

Figure S-5. ESI-MS spectra of (a) d18:1/C24:1 ST and **(**b) d18:1/C24:0 ST recorded for samples deposited on aluminum foil and kept in a darkroom at times 0, 1 h and 1 day under sufficient airflow. One hundred pmol of each sample was loaded on the aluminum foil. After being maintained for fixed times in the darkness, the STs were extracted with 100 µL of solvent mixture isopropyl alcohol/methanol/water (9:1:1, v/v/v) and were analyzed directly by ESI-MS.

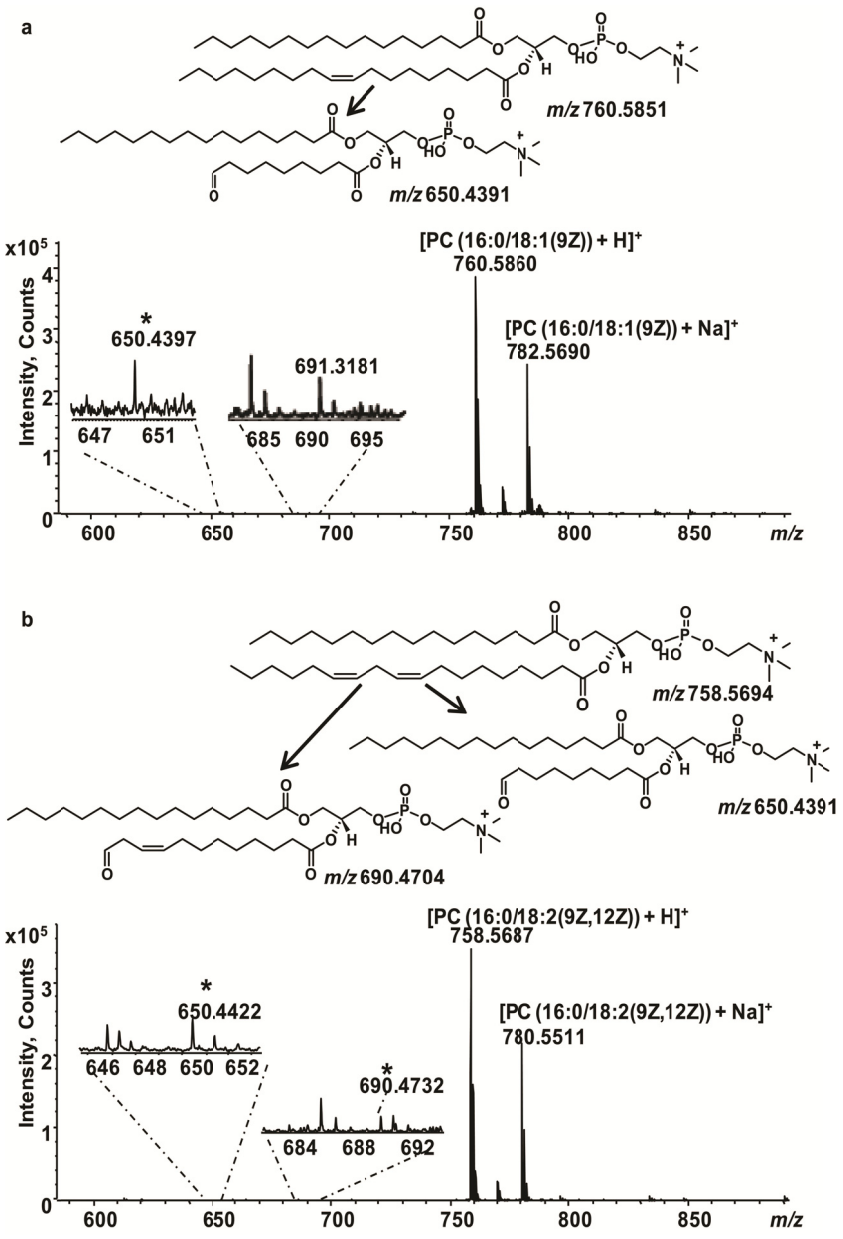

Figure S-6. Positive-ion MS spectra of phosphatidylcholine (a) (16:0/18:1(9Z)) and (b) (16:0/18:2(9Z, 12Z)) deposited on aluminum foil and exposed to the ambient air for 20 min. Oxidation products are labeled with an asterisk (*).

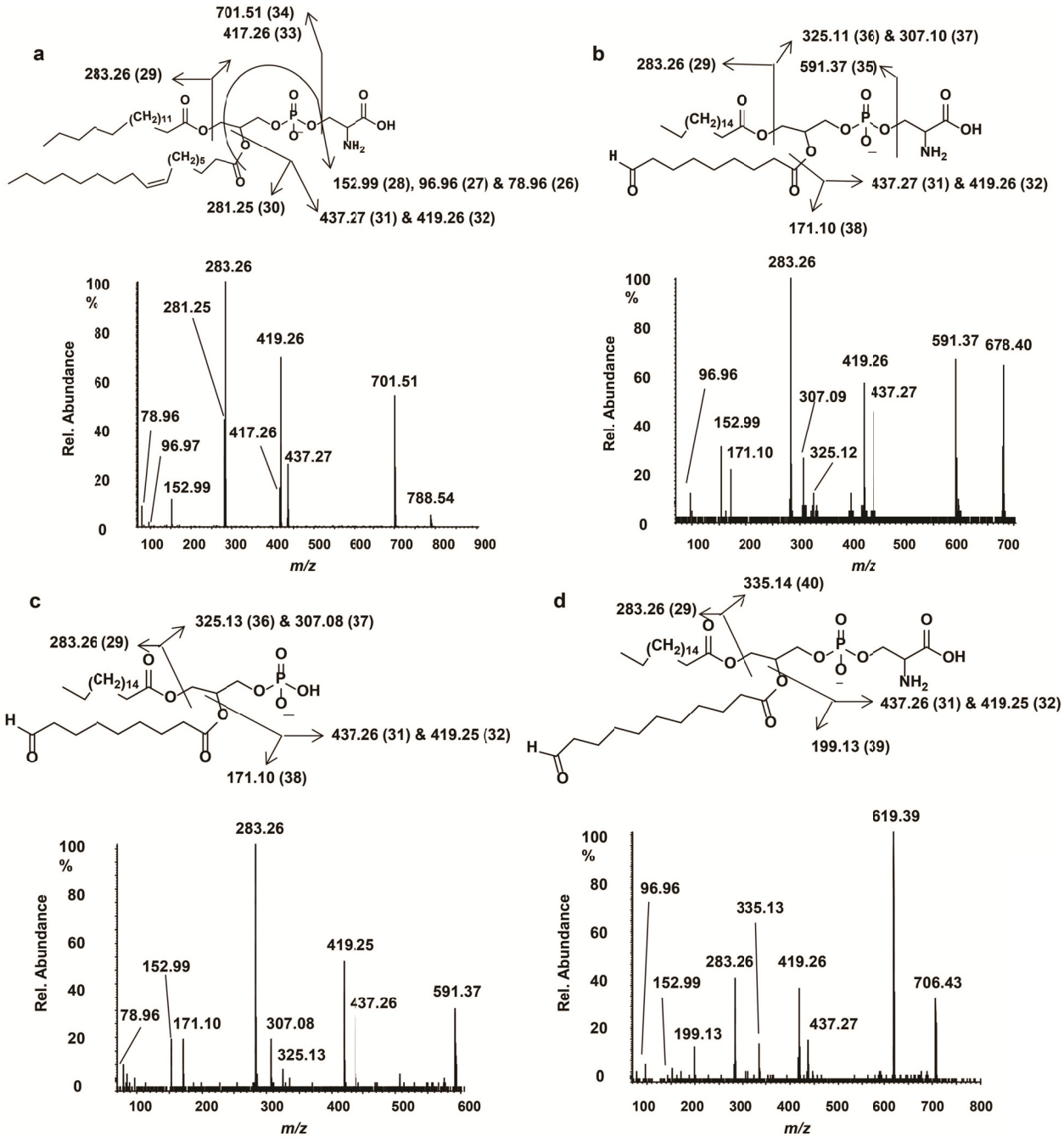

Figure S-7. Negative-ion CID MS/MS spectra of PS candidates and their oxidation products recorded after the bovine brain total lipid extracts were separated by TLC and exposed to ambient air. Spectra were assigned as (a) PS (18:0/18:1), $[M - H]^-$ *m/z* 788.54; (b) PS (18:0/9:1[O]) aldehyde, $[M - H]^-$ *m/z* 678.40; (c) PA (18:0/9:1[O]) aldehyde, $[M - H]^-$ *m/z* 591.37 and (d) PS (18:0/11:1[O]) aldehyde, $[M - H]^-$ *m/z* 706.43. Structures of the CID fragments are shown in the structure list in Figure S-11.

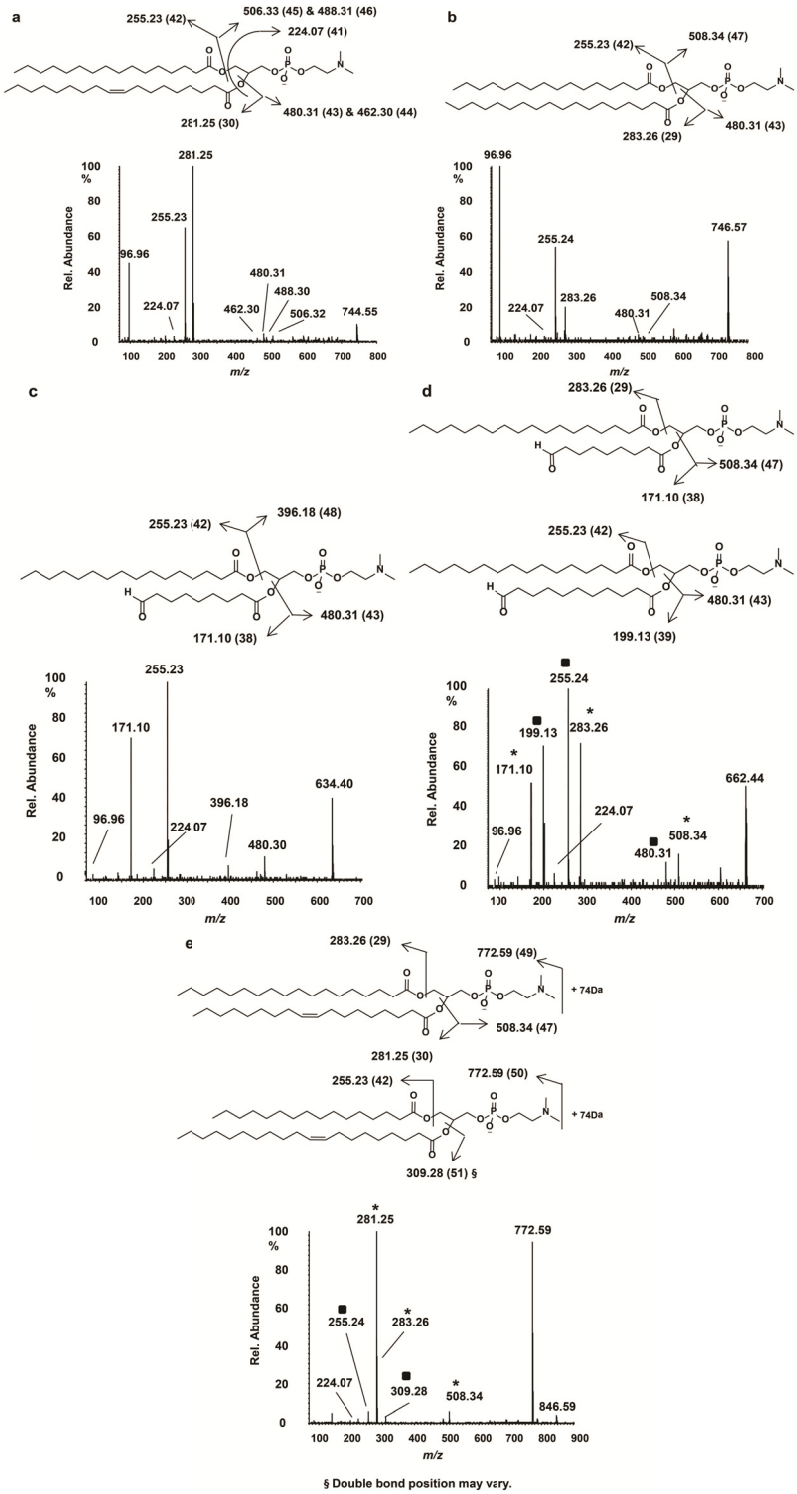

Figure S-8. CID spectra of precursor ions that represent potential PE-NMe_2 lipids and their oxidation products collected after the bovine brain total lipid extract was separated by TLC and exposed to ambient air. Spectra were assigned as (a) PE-NMe_2 (16:0/18:1), (b) PE-NMe_2 (16:0/18:0), (c) PE-NMe_2 (16:0/9:1[O]) aldehyde, (d) PE-NMe_2 (16:0/11:1[O]) aldehyde and (e) mixture of PE-NMe_2 (16:0/20:1) and PE-NMe_2 (18:0/18:1) with the easily dissociated adduct of

74 Da that may correspond to a glyceryl ester on the phosphate or an experimental artifact. The asterisk (*) and black square (■), respectively, indicate fragments from the different precursor ion sources. Structures of the CID fragments are shown in the structure list in Figure S-11.

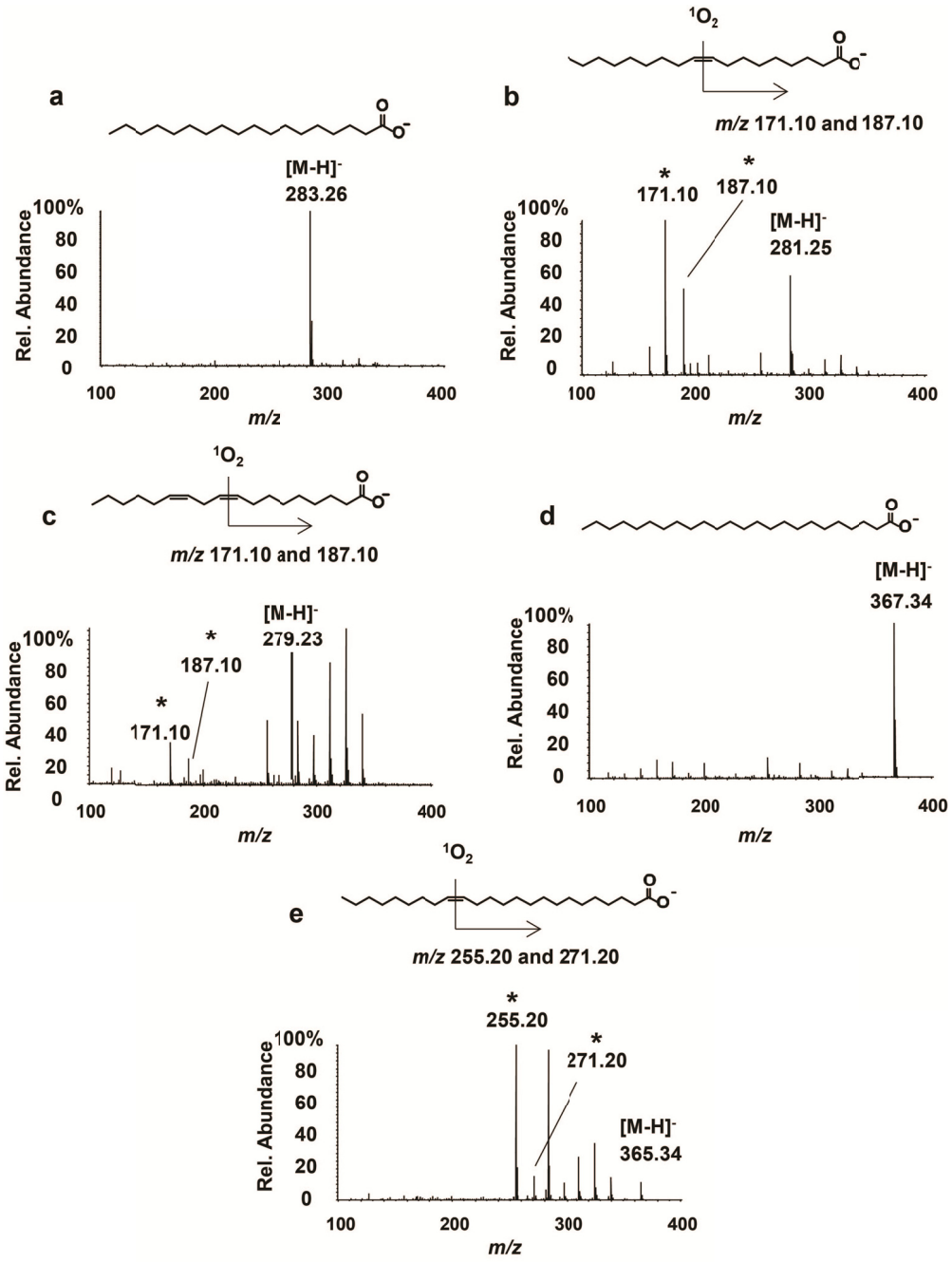

Figure S-9. Negative-ion mode ESI-MS spectra of fatty acids deposited on aluminum foil and exposed to the ambient air for 1 h. (a) stearic acid C18:0, (b) oleic acid C18:1 (9*Z*), (c) linoleic acid C18:2 (9*Z*, 12*Z*), (d) lignoceric acid C24:0 and (e) nervonic acid C24:1 (15*Z*).

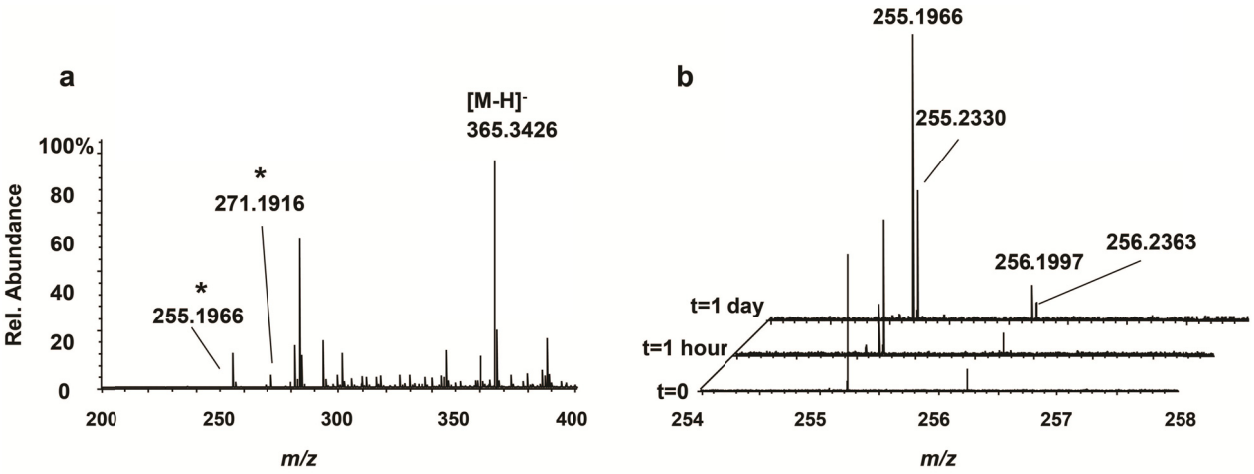

Figure S-10. FT MS spectrum acquired following deposition of 100 pmol nervonic acid C24:1 (15*Z*) on aluminum foil and exposure under ambient laboratory air for 1 h. The high resolution spectrum (M/ΔM 60,000 at *m/z* 400) was obtained with a 12-T SolariX instrument (Bruker Daltonics Inc., Billerica, MA, USA) using a modified Bruker nanoelectrospray source. (a) FT MS spectrum obtained after 1-h exposure to the air. (b) Zoomed–in FT MS spectra shown in the mass range *m/z* 254~258 over time. Herein, separation of the signal of the aldehyde product (*m/z* 255.1966) from the background (*m/z* 255.2330) is clear.

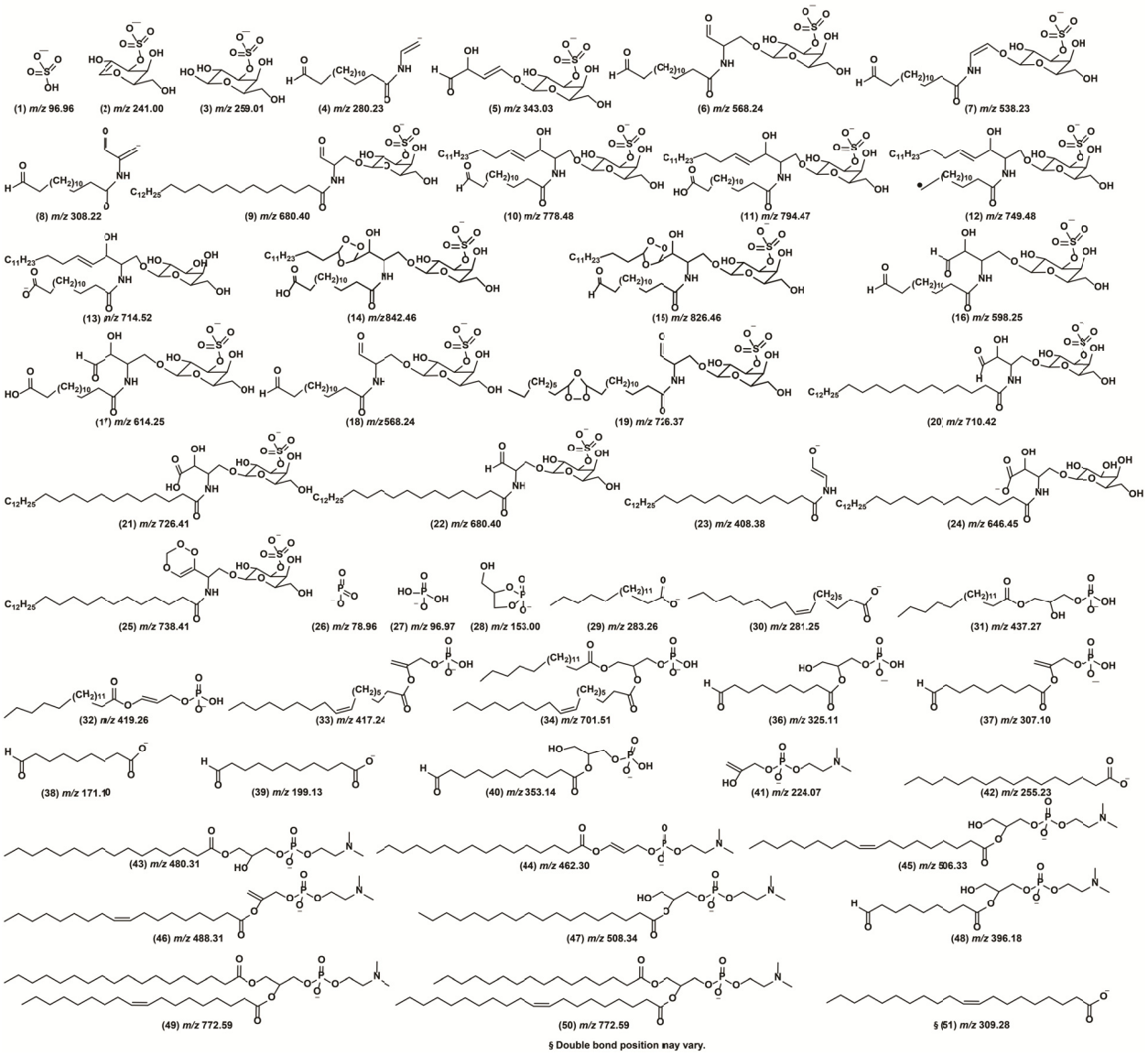

Figure S-11. Proposed structures of fragments observed in CID spectra shown in the supplementary materials.

References:

(1) Harrison, K. A.; Murphy, R. C. *Anal. Chem.* **1996**, *68*, 3224.

(2) Stokes, G. Y.; Buchbinder, A. M.; Gibbs-Davis, J. M.; Scheidt, K. A.; Geiger, F. M. *J. Phys. Chem. A* **2008**, *112*, 11688.

(3) Baptista, L.; Pfeifer, R.; da Silva, E. C.; Arbilla, G. *J. Phys. Chem. A* **2011**, *115*, 10911.